

Using Demand Response to Improve Power System Voltage Stability Margins

Mengqi Yao
Johanna L. Mathieu
Electrical and Computer Engineering
University of Michigan
Ann Arbor, Michigan, USA
{mqyao; jlmath}@umich.edu

Daniel K. Molzahn
Energy Systems Division
Argonne National Laboratory
Lemont, Illinois, USA
dmolzahn@anl.gov

Abstract—Electric power systems with high penetrations of fluctuating renewable generation may operate close to their stability limits. Demand response can be used to improve power system stability. For example, it is already used to provide frequency control, improving frequency stability. This paper presents a new demand response strategy that uses fast-acting flexible loads to change the loading pattern while keeping the total load constant, improving steady-state voltage stability without affecting the system frequency. The new loading pattern is maintained only for a short period of time until the generators can be re-dispatched. Our goal is to find a permissible loading pattern that maximizes the smallest singular value of the power flow Jacobian matrix, which serves as a measure of voltage stability. The corresponding non-convex optimization problem is solved with an iterative linear programming approach that uses eigenvalue sensitivities and a linearization of the AC power flow equations. Using two IEEE test cases as illustrative examples, we show that the loading patterns resulting from the proposed approach give smallest singular values that are very close to those obtained from a brute force search. The results are also compared to another voltage stability measure given by the maximum loading margin for uniformly varying power injections.

Index Terms—demand response, eigenvalue sensitivity, optimization, power system stability margin, smallest singular value

I. INTRODUCTION

Electric power system stability refers to the ability to operate normally after a disturbance [1]. Fluctuating renewable generation may result in operation close to the system’s stability limits. Conventional methods to improve power system stability include generator re-dispatch and use of Flexible AC Transmission System and/or other power electronic devices [2]–[4]. Demand Response (DR) can also be used to improve power system stability. Most of the relevant research, e.g., [5], [6], has focused on using flexible loads to improve frequency stability by time shifting their aggregate energy consumption to help balance supply and demand.

DR could also be used to improve steady-state voltage stability margins, which estimate how far a specified operating point is from instability due to voltage collapse. This paper considers two types of voltage stability margins. The first is the

smallest singular value of the power flow Jacobian matrix [7]–[10]. The smallest singular value gives us a measure of how close the Jacobian is to being singular, i.e., power flow infeasibility. Feasibility and stability are closely linked [11]. The second, termed the loading margin, is the distance between the current operating point and the maximum loading point, assuming that load and generation are increased uniformly (in a multiplicative sense) throughout the system [2]. The loading margin is calculated using a Continuation Power Flow to compute the distance to the instability.

Generation and load levels affect voltage stability margins. In order to maintain reliability, control actions are required when a system’s operating point provides insufficient stability margins. Generator re-dispatch takes time because of generator ramp limits. In contrast, flexible loads coordinated to provide DR via low-latency communication systems can respond more quickly. Rather than shifting load in time, we propose to improve voltage stability margins by shifting load in space – simultaneously decreasing some loads while increasing others – such that total load is constant and the system frequency is unaffected.¹ The new loading pattern should only be maintained for a short period of time until the generators can be re-dispatched. This should be followed by a period in which the loads that decreased consumption consume more and the loads that increased consumption consume less in order to “pay back” the energy consumed/not consumed previously.

This paper presents a method for computing a loading pattern that maximizes the smallest singular value of the power flow Jacobian matrix. We formulate a non-convex optimization problem that maximizes this quantity subject to the AC power flow equations, line limits, voltage magnitude limits, generator reactive power limits, and a constraint that forces the total loading to be unchanged. To solve this problem, we use an iterative linear programming approach that employs eigenvalue sensitivities and a linearization of the AC power flow equations. Eigenvalue sensitivities have also been used to design damping controllers in power systems [12]–[14].

The main contributions of this paper are 1) the formulation

Support from NSF Grant EECS-1549670 and the U.S. DOE, Office of Electricity Delivery and Energy Reliability under contract DE-AC02-06CH11357.

¹Although, in practice, primary frequency control will manage small load deviations, we choose to require total load to remain constant to isolate the impact of load pattern changes from changes in the total loading.

of a non-convex optimization problem to choose loading patterns that maximize the smallest singular value of the power flow Jacobian, 2) a computationally tractable algorithm to solve this problem, 3) case studies using the IEEE 9- and 30-bus test systems to assess algorithmic performance, and 4) comparison of the solutions given by the algorithm with those of three benchmark approaches – one using a brute force search and two that maximize the loading margin.

This paper is structured as follows: Section II describes the problem and details our assumptions. Section III presents the smallest singular value maximization problem formulation and solution algorithm. Section IV shows the results of our case studies and Section V concludes the paper.

II. PROBLEM DESCRIPTION & ASSUMPTIONS

A conceptual illustration of the problem is shown in Fig. 1. The shaded region is the feasible space and the purple cross is the initial stable operating point. A disturbance may cause the operating point to move towards the feasibility boundary (i.e., to the red diamond, step 1). Our goal is to determine a new load pattern to move the operating point away from the boundary (e.g., to the green square, step 2). We require the total flexible load (from e.g., air conditioners, electric vehicles) to remain constant, so as not to affect the system frequency. We assume that, initially, generator real power outputs are fixed with the exception of the slack generator which compensates for the change in losses associated the new loading pattern. (Note that it would also be possible to use a distributed slack.) Generator reactive power outputs adjust to the new loading pattern. After a short period of time, the generators are re-dispatched so that the flexible loads can return to consuming their nominal demands plus/minus some power to “pay back” the energy consumed/not consumed during their DR actions. Again, the operating point changes; for example, it could return to the initial operating point (step 3), or another point with an adequate stability margin. In this paper, we develop a method to achieve step 2 in Fig. 1 – choosing a new loading pattern to improve the stability margin (but not necessarily reach the maximum point) – and leave step 3 for future work.

We assume flexible load exists at some or all PQ buses in a network and, for simplicity, assume that the entire load at the bus is flexible. Constraining the load flexibility within our optimization problems is straightforward and does not change the problem complexity. We model all PQ buses as constant power factor loads. In the future, we will explore the impact of including ZIP load and motor load models. We also model all generation buses (except the slack bus) as PV buses, and so assume their voltage magnitudes are fixed since automatic voltage regulators respond in sub-second time frames.²

²Reactive power generation constraints in our formulation preclude the need to consider PV/PQ bus switching due to reactive power limits. Future work will investigate the potential impact from the additional flexibility afforded by a more general generator model that allows the voltage magnitude to change upon reaching a reactive generation limit.

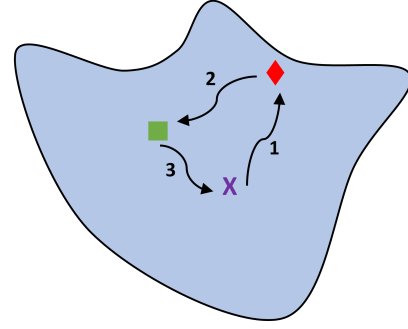


Fig. 1. Conceptual illustration of the problem.

III. OPTIMIZATION APPROACH

After summarizing our notation, this section describes the non-convex optimization problem for maximizing the smallest singular value of the power flow Jacobian. This section then formulates the iterative linear programming algorithm used to solve this non-convex problem, including the derivation of eigenvalue sensitivities. Finally, this section summarizes alternative voltage stability margins which serve as benchmarks.

A. Notation

Variables & Parameters

θ_n	Voltage angle at bus n
V_n	Voltage magnitude at bus n
$J(\boldsymbol{\theta}, \mathbf{V})$	Jacobian matrix
$P_{g,n}$	Real power generation at bus n
$P_{d,n}$	Real power demand at bus n
$Q_{g,n}$	Reactive power generation at bus n
$Q_{d,n}$	Reactive power demand at bus n
ε_0	Total flexible load
$\varepsilon_{g,n}$	Previous real power generation at bus n
$\varepsilon_{d,n}$	Previous real power demand at bus n
β_n	Previous voltage magnitude at bus n
μ_n	Ratio between real and reactive demand at bus n
κ_{nm}	Apparent power line limit for line (n, m)
λ	Eigenvalue of a matrix
u	Normalized right eigenvector
w	Normalized left eigenvector
γ	Loading factor

Functions

$\mathcal{F}_n^P(\cdot)$	Real power injection at bus n
$\mathcal{F}_n^Q(\cdot)$	Reactive power injection at bus n
$\mathcal{H}_{nm}(\cdot)$	Line flow for line (n, m)
$f_n^P(\cdot)$	Linearization of \mathcal{F}_n^P
$f_n^Q(\cdot)$	Linearization of \mathcal{F}_n^Q
$h_{nm}(\cdot)$	Linearization of \mathcal{H}_{nm}

Sets

\mathcal{N}	Set of all buses
\mathcal{S}_{PV}	Set of all PV buses
\mathcal{S}_{PQ}	Set of all PQ buses
\mathcal{S}_{DR}	Set of buses with flexible loads

Bold symbols denote vectors including all variables of a type. Overlines and underlines represent the upper and lower

limits for a variable. Subscript ‘ref’ denotes the slack bus. Superscript ‘ T ’ denotes the transpose of a matrix. The notation $X \succeq 0$ means that X is a positive semidefinite matrix.

B. Smallest Singular Value Maximization Problem

The goal of the optimization problem is to find the operating point that maximizes the smallest singular value of the power flow Jacobian matrix $J(\boldsymbol{\theta}, \mathbf{V})$. Because the singular values of a matrix A are the square roots of the eigenvalues of $A^T A$, an equivalent problem is to maximize the smallest eigenvalue λ_0 of the matrix $J(\boldsymbol{\theta}, \mathbf{V})^T J(\boldsymbol{\theta}, \mathbf{V})$. Therefore, we formulate the optimization problem as follows.

$$\max_{\substack{P_g, Q_g, P_d, \\ Q_d, \mathbf{V}, \theta, \lambda_0}} \lambda_0 \quad \text{subject to} \quad (1a)$$

$$J(\boldsymbol{\theta}, \mathbf{V})^T J(\boldsymbol{\theta}, \mathbf{V}) - \lambda_0 I \succeq 0 \quad (1b)$$

$$F_n^P(\boldsymbol{\theta}, \mathbf{V}) = P_{g,n} - P_{d,n} \quad \forall n \in \mathcal{N} \quad (1c)$$

$$F_n^Q(\boldsymbol{\theta}, \mathbf{V}) = Q_{g,n} - Q_{d,n} \quad \forall n \in \mathcal{N} \quad (1d)$$

$$\sum_{n \in \mathcal{S}_{\text{DR}}} P_{d,n} = \varepsilon_0 \quad (1e)$$

$$P_{d,n} \cdot \mu_n = Q_{d,n} \quad \forall n \in \mathcal{S}_{\text{PQ}} \quad (1f)$$

$$P_{d,n} = \varepsilon_{d,n} \quad \forall n \in \mathcal{S}_{\text{PQ}} \setminus \mathcal{S}_{\text{DR}} \quad (1g)$$

$$P_{g,n} = \varepsilon_{g,n} \quad \forall n \in \mathcal{S}_{\text{PV}} \quad (1h)$$

$$V_n = \beta_n \quad \forall n \in \mathcal{S}_{\text{PV}} \quad (1i)$$

$$V_{\text{ref}} = 1, \theta_{\text{ref}} = 0 \quad (1j)$$

$$\mathcal{H}_{nm}(\boldsymbol{\theta}, \mathbf{V}) \leq \kappa_{nm} \quad (1k)$$

$$\mathcal{H}_{mn}(\boldsymbol{\theta}, \mathbf{V}) \leq \kappa_{mn} \quad (1l)$$

$$\underline{P}_{g,\text{ref}} \leq P_{g,\text{ref}} \leq \overline{P}_{g,\text{ref}} \quad (1m)$$

$$\underline{Q}_{g,\text{ref}} \leq Q_{g,\text{ref}} \leq \overline{Q}_{g,\text{ref}} \quad (1n)$$

$$\underline{Q}_{g,n} \leq Q_{g,n} \leq \overline{Q}_{g,n} \quad \forall n \in \mathcal{S}_{\text{PV}} \quad (1o)$$

$$\underline{V}_n \leq V_n \leq \overline{V}_n \quad \forall n \in \mathcal{S}_{\text{PQ}} \quad (1p)$$

In this problem, we choose P_d to maximize λ_0 , where Q_g is also free to change. In combination with the objective function (1a), the semidefinite constraint (1b) forces λ_0 to be the smallest eigenvalue of $J(\boldsymbol{\theta}, \mathbf{V})^T J(\boldsymbol{\theta}, \mathbf{V})$, where I is an identity matrix of appropriate size. Constraints (1c) and (1d) are the nonlinear AC power flow equations [15], (1e) ensures that the total flexible load remains constant, (1f) models loads as constant power factor demands, and (1g)–(1i) constrain the inflexible loads’ real power consumption, the generators’ real power production, and voltage magnitudes at the PV buses to remain fixed at their previous values. Constraint (1j) sets the slack bus voltage magnitude and angle and (1k)–(1p) limit the line flows, real and reactive power generation at the slack bus, reactive power generation at PV buses, and voltage magnitudes at PQ buses.

While we could apply a semidefinite relaxation of the AC power flow equations [16], [17] and solve the problem with semidefinite programming (SDP), we are not guaranteed to obtain the actual solution, only a lower bound. Therefore, we reformulate the problem using linear eigenvalue sensitivities to replace (1b) and linearized AC power flow equations to replace (1c)–(1d) so that we can apply iterative linear programming. Future work includes analyzing the SDP relaxation of (1).

C. Linear Eigenvalue Sensitivities

Let λ_i , u_i and w_i be the eigenvalues, normalized right eigenvectors, and normalized left eigenvectors of a matrix A :

$$A u_i = \lambda_i u_i \quad (2)$$

$$A^T w_i = \lambda_i w_i \quad (3)$$

Differentiating (2) with respect to a system parameter ξ yields

$$\frac{\partial A}{\partial \xi} u_i + A \frac{\partial u_i}{\partial \xi} = \frac{\partial \lambda_i}{\partial \xi} u_i + \lambda_i \frac{\partial u_i}{\partial \xi} \quad (4)$$

Pre-multiplying (4) by w_i^T , applying (3), and using the fact that w_i and u_i are orthogonal ($w_i^T u_i = 1$), the eigenvalue sensitivity is [18]:

$$\frac{\partial \lambda_i}{\partial \xi} = w_i^T \frac{\partial A}{\partial \xi} u_i \quad (5)$$

Since the Jacobian depends on θ and V , let

$$\xi = [\theta_1, \dots, \theta_i, V_1, \dots, V_j]^T \quad \forall i \in \mathcal{S}_{\text{PV}}, \mathcal{S}_{\text{PQ}}, \forall j \in \mathcal{S}_{\text{PQ}} \quad (6)$$

and so we can approximate the change in λ_0 as

$$\Delta \lambda_0 = \sum_i \left[w_0^T \frac{\partial(J^T J)}{\partial \theta_i} u_0 \right] \Delta \theta_i + \sum_j \left[w_0^T \frac{\partial(J^T J)}{\partial V_j} u_0 \right] \Delta V_j \quad (7)$$

where u_0 and w_0 are the normalized right and left eigenvectors corresponding to λ_0 .

D. Iterative Linear Programming Problem

In addition to using the linear eigenvalue sensitivity (7), we also linearize the AC power flow equations so that we can use iterative linear programming [15, p. 371]. Assume a previous power flow solution: P_g^0 , Q_g^0 , P_d^0 , Q_d^0 , θ^0 , and V^0 . In each iteration, the optimization goal is to choose $\Delta P_d, \Delta Q_d, \Delta \theta$, and ΔV :

$$\max_{\substack{\Delta P_g, \Delta Q_g, \Delta P_d, \\ \Delta Q_d, \Delta V, \Delta \theta, \Delta \lambda_0}} \Delta \lambda_0 \quad \text{subject to} \quad (8a)$$

$$\text{constraint (7)} \quad (8b)$$

$$f_n^P(\Delta \theta, \Delta V) = \Delta P_{g,n} - \Delta P_{d,n} \quad \forall n \in \mathcal{N} \quad (8c)$$

$$f_n^Q(\Delta \theta, \Delta V) = \Delta Q_{g,n} - \Delta Q_{d,n} \quad \forall n \in \mathcal{N} \quad (8d)$$

$$\sum_{n \in \mathcal{S}_{\text{DR}}} \Delta P_{d,n} = 0 \quad (8e)$$

$$\Delta P_{d,n} \cdot \mu_n = \Delta Q_{d,n} \quad \forall n \in \mathcal{S}_{\text{PQ}} \quad (8f)$$

$$\Delta P_{d,n} = 0 \quad \forall n \in \mathcal{S}_{\text{PQ}} \setminus \mathcal{S}_{\text{DR}} \quad (8g)$$

$$\Delta P_{g,n} = 0 \quad \forall n \in \mathcal{S}_{\text{PV}} \quad (8h)$$

$$\Delta V_n = 0 \quad \forall n \in \mathcal{S}_{\text{PV}} \quad (8i)$$

$$\Delta V_{\text{ref}} = 0, \Delta \theta_{\text{ref}} = 0 \quad (8j)$$

$$h_{nm}(\Delta \theta, \Delta V) \leq \kappa_{nm} \quad (8k)$$

$$h_{mn}(\Delta \theta, \Delta V) \leq \kappa_{mn} \quad (8l)$$

$$\underline{P}_{g,\text{ref}} \leq \Delta P_{g,\text{ref}} + P_{g,\text{ref}}^0 \leq \overline{P}_{g,\text{ref}} \quad (8m)$$

$$\underline{Q}_{g,\text{ref}} \leq \Delta Q_{g,\text{ref}} + Q_{g,\text{ref}}^0 \leq \overline{Q}_{g,\text{ref}} \quad (8n)$$

$$\underline{Q}_{g,n} \leq \Delta Q_{g,n} + Q_{g,n}^0 \leq \overline{Q}_{g,n} \quad \forall n \in \mathcal{S}_{\text{PV}} \quad (8o)$$

$$\underline{V}_n \leq \Delta V_n + V_n^0 \leq \bar{V}_n \quad \forall n \in \mathcal{S}_{PQ} \quad (8p)$$

$$\Delta \lambda_0 \leq \overline{\Delta \lambda}_0 \quad (8q)$$

where (8b) is the linear eigenvalue sensitivity constraint, (8c)–(8p) correspond to (1c)–(1p), and (8q) limits the maximum change in $\Delta \lambda_0$ since the linearizations are only valid near the previous operating point. After obtaining a solution to (8) and before the next iteration, P_g^0 , Q_g^0 , P_d^0 , Q_d^0 , θ^0 , and V^0 are updated by adding ΔP_g , ΔQ_g , ΔP_d , ΔQ_d , $\Delta \theta$, and ΔV , respectively; the AC power flow is re-solved; and the linearizations (8b)–(8d) and (8k)–(8l) are re-computed for the new operating point. Iterations are terminated when $\Delta \lambda_0$ goes below a threshold (here, we use 10^{-5}).

E. Benchmarks

We refer to (8) as the *iterative sensitivity smallest singular value (SSV) approach* and benchmark its solution against those of three other approaches.

1) *Brute force SSV approach*: We compute the smallest singular value of the Jacobian for all possible loading patterns within a discrete mesh where total load is constant (i.e., using brute force search) and determine the maximum.

2) *Brute force loading margin approach*: We use MATPOWER's [19] continuation power flow `runcpf` to compute the loading margin for all possible loading patterns within a discrete mesh where total load is constant and determine the maximum. This function does not enforce engineering constraints.

3) *Optimal loading margin approach*: For all possible loading patterns where total load is constant, we use an Optimal-Power-Flow-based Direct Method [20] to maximize the loading factor γ subject to both the power flow equations and engineering constraints. Specifically, we solve the following problem, which increases the generation and loading uniformly subject to the power flow equations and engineering constraints:

$$\max_{P_g, Q_g, P_d, Q_d, V, \theta, \gamma} \gamma \quad \text{subject to} \quad (9a)$$

$$P_{g,n} = (1 + \gamma)P_{g,n}^0 \quad \forall n \in \mathcal{S}_{PV} \quad (9b)$$

$$P_{d,n} = (1 + \gamma)P_{d,n}^0 \quad \forall n \in \mathcal{S}_{PQ} \quad (9c)$$

$$\sum_{n \in \mathcal{S}_{DR}} P_{d,n}^0 = \varepsilon_0 \quad (9d)$$

$$P_{d,n}^0 = \varepsilon_{d,n} \quad \forall n \in \mathcal{S}_{PQ} \setminus \mathcal{S}_{DR} \quad (9e)$$

$$P_{g,n}^0 = \varepsilon_{g,n} \quad \forall n \in \mathcal{S}_{PV} \quad (9f)$$

$$\text{constraints (1c), (1d), (1f), (1i)–(1p)} \quad (9g)$$

where $P_{g,n}^0$ and $P_{d,n}^0$ define the base operating point.

IV. RESULTS

We next demonstrate the performance of our iterative sensitivity SSV approach on the IEEE 9- and 30-bus systems. We use these small-scale systems to enable visualization of the results. The approach is also expected to be applicable to large-scale systems, which we will verify in future work. We use the system data from MATPOWER [19] and set $\overline{\Delta \lambda}_0 = 0.001$.

TABLE I
COMPARISON BETWEEN ORIGINAL OPTIMAL POWER FLOW SOLUTION AND SOLUTION TO (8) FOR THE 9-BUS SYSTEM

Bus #	Original Generation		New Generation	
	P_g (MW)	Q_g (MVar)	P_g (MW)	Q_g (MVar)
1	71.95	24.07	70.18	3.05
2	163	14.46	163	19.5
3	85	-3.65	85	3.13
Bus #	Original Load/Voltage		New Load/Voltage	
	P_d (MW)	V (p.u.)	P_d (MW)	V (p.u.)
5	90	0.975	74.8	0.989
7	100	0.986	166.68	0.966
9	125	0.958	73.52	0.985

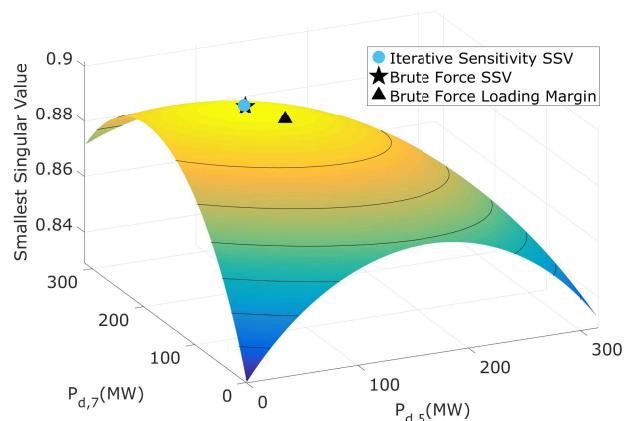


Fig. 2. Smallest singular value of the power flow Jacobian for the 9-bus system as a function of $P_{d,5}$ and $P_{d,7}$.

A. Nine-bus System

We assume the loads at buses 5, 7 and 9 are flexible (total loading = flexible loading = 315 MW). A comparison between the original optimal power flow solution and the solution to (8) is given in Table I. As specified by the constraints, the real power generation at buses 2 and 3 does not change, while the load pattern P_d and the slack bus generation changes to maximize the smallest singular value of the power flow Jacobian, which increases from 0.8942 to 0.8995.

To verify the results, we compare the solution of the iterative sensitivity SSV approach to that of the brute force SSV approach. Figure 2 shows the SSV as a function of $P_{d,5}$ and $P_{d,7}$ (based on (8e), $P_{d,9} = 315 - P_{d,5} - P_{d,7}$ MW), using a mesh size of 1 MW. The solution of the iterative sensitivity SSV approach is very near to that of the brute force SSV approach, which has a maximum value that is only 0.00001% larger than that of the iterative sensitivity SSV approach.

Figure 3 shows the loading margin as a function of $P_{d,5}$ and $P_{d,7}$. The solutions of the brute force and optimal loading margin approaches are shown. Both approaches produce similar loading patterns (the black dashed line projects the loading pattern corresponding to the optimal loading margin approach to the surface), but different loading margins since the optimal approach includes engineering constraints that reduce the margin from 566 to 257 MW.

Table II summarizes the results by listing the loading

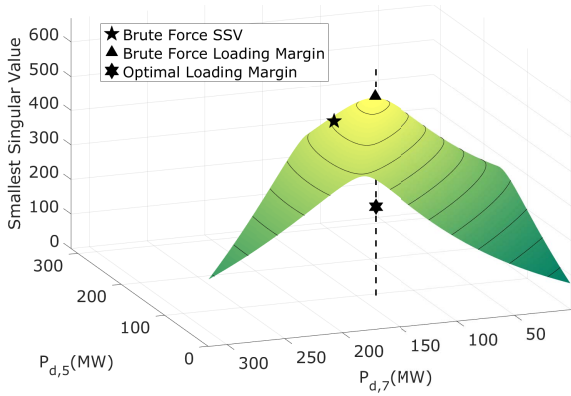


Fig. 3. Loading margin for the 9-bus system as a function of $P_{d,5}$ and $P_{d,7}$.

TABLE II
OPTIMAL LOADING PATTERNS FOR THE 9-BUS SYSTEM

Approach	$P_{d,5}$	$P_{d,7}$	$P_{d,9}$	SSV	LM
Brute Force SSV	76	167	72	0.8995	516
Iterative Sensitivity SSV	75	167	73	0.8995	516
Brute Force Loading Margin	97	135	83	0.8984	566
Optimal Loading Margin	95	135	85	0.8984	257

patterns, smallest singular values (SSV), and loading margins (LM) produced by each approach. Note that the loading margins reported for the first two approaches are computed without engineering constraints and so should be compared to the loading margin associated with the brute force loading margin approach. As shown, the loading patterns produced by the loading margin approaches are different than those produced by the SSV approaches. This is unsurprising since the margins are defined differently,³ but it points to the issue that improving one margin may come at the cost of reducing another.

B. Thirty-bus System

We assume the loads at buses 7, 8 and 30 are flexible (63.4 MW out of 189.2 MW total). A comparison between the original optimal power flow solution and the solution to (8) is given in Table III. Figure 4 shows the SSVs (again, using a mesh size of 1 MW) and solutions of two SSV approaches, and Fig. 5 shows the loading margins and the solutions of two loading margin approaches. In both cases, the results are plotted as a function of $P_{d,7}$ and $P_{d,8}$, and so, based on (8e), $P_{d,30} = 63.4 - P_{d,7} - P_{d,8}$. Table IV summarizes the results.

As shown in Fig. 4 and Table IV, the result from the iterative sensitivity SSV approach is near the actual maximum. Along the line $P_7 + P_8 = 63$, the smallest singular value slightly increases (from 0.2171 to 0.2187) as the load at bus 7 increases. As shown in Fig. 5 and Table IV, the loading margin associated with the solution of the optimal loading margin approach is much smaller than that associated with the brute force loading margin approach, again due to the engineering constraints; however, the loading pattern is similar. Also, again, the SSV approaches produce very different loading patterns than the loading margin approaches.

³In particular, the loading margin describes the distance to voltage instability for power injection changes that are restricted to a single profile (i.e., uniform changes at constant power factor), whereas the smallest singular value does not require specification of a power injection profile.

TABLE III
COMPARISON BETWEEN ORIGINAL OPTIMAL POWER FLOW SOLUTION AND SOLUTION TO (8) FOR THE 30-BUS SYSTEM

Bus #	Original Generation		New Generation	
	P_g (MW)	Q_g (MVar)	P_g (MW)	Q_g (MVar)
1	25.82	-2.46	26.40	-2.87
2	60.97	25.75	60.97	32.27
13	37	10.62	37.00	10.92
22	21.59	37.56	21.59	38.69
23	19.2	7.59	19.20	7.70
27	26.91	8.29	26.91	4.62

Bus #	Original Load/Voltage		New Load/Voltage	
	P_d (MW)	V (p.u.)	P_d (MW)	V (p.u.)
7	22.8	0.971	57.52	0.951
8	30	0.970	5.88	0.978
30	10.6	0.971	0	0.996

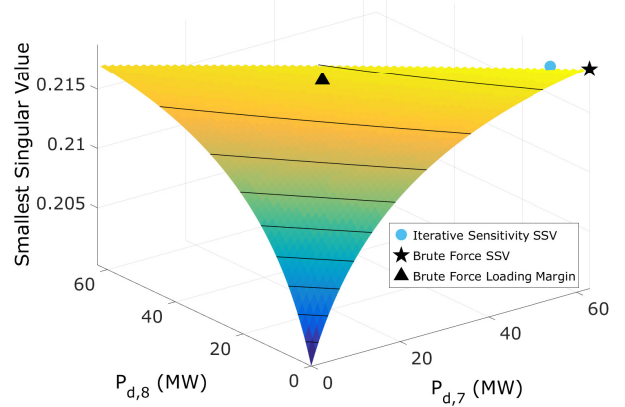


Fig. 4. Smallest singular value of the power flow Jacobian for the 30-bus system as a function of $P_{d,7}$ and $P_{d,8}$.

Figure 6 shows the convergence of the iterative sensitivity SSV approach to the optimal point. Less than 25 iterations are needed for convergence of the 9-bus system and 40 iterations for the 30-bus system. Using MATLAB on an Intel(R) i7-4720HQ CPU with 16 GB of RAM, the solution for the 30-bus system is obtained in less than 1 seconds.

The overall computation time is a function of the number of iterations needed and the time required for each iteration, where the former depends on the initial operating point and the step size $\Delta\lambda_0$ and the latter depends on the size of Jacobian matrix ($m \times m$). The time complexity to compute (7) is $O(m^3)$. Applying the algorithm to the IEEE 118-bus system resulted in a computation time of 15 seconds though it could be reduced, e.g., through parallel computing. In both Fig. 2 and Fig. 4, we can see that the smallest singular value is relatively constant near the maximum. If this result generalizes to other systems, we do not need to wait until the iterative sensitivity SSV algorithm fully converges to obtain a good solution.

V. CONCLUSIONS AND FUTURE WORK

This paper has proposed a method for using demand response to improve steady-state voltage stability margins. Specifically, we formulated an optimization problem that seeks the loading pattern that maximizes the smallest singular value

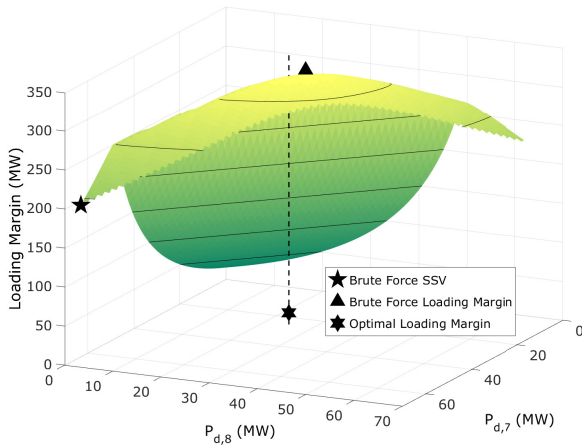


Fig. 5. Loading margin for the 30-bus system as a function of $P_{d,7}$ and $P_{d,8}$.

TABLE IV
OPTIMAL LOADING PATTERNS FOR THE 30-BUS SYSTEM

Approach	$P_{d,7}$	$P_{d,8}$	$P_{d,30}$	SSV	LM
Brute Force SSV	63	0	0	0.2187	194
Iterative Sensitivity SSV	58	6	0	0.2187	209
Brute Force Loading Margin	24	28	11	0.2173	323
Optimal Loading Margin	25	25	13	0.2172	15

of the power flow Jacobian, which serves as a voltage stability margin. To solve this optimization problem, we proposed an iterative linear programming algorithm using eigenvalue sensitivities and a linearization of the AC power flow equations. We applied the method to two test systems and benchmarked its performance against a brute force approach and two approaches that maximize the loading margin.

The test case results show that demand response actions which shift load between buses, while keeping the total load constant, can improve voltage stability margins. We also found that our computationally tractable iterative linear programming method produced loading patterns close to the optimum (as determined by a brute force approach). The results further show that we may obtain significantly different loading patterns when maximizing the smallest singular value of the Jacobian versus maximizing the loading margin. This is not surprising since the different margins capture different notions of “distance to instability.” However, it means that improving one margin may worsen another, and so the system operator should consider the trade-off between different margins.

Future work includes analyzing the convergence of the iterative linear programming method, developing strategies for re-dispatching the system to compensate for the DR actions while keeping the system away from its stability boundaries, and investigating related optimization formulations using other stability margins, including dynamic stability margins.

REFERENCES

[1] P. Kundur, J. Paserba, V. Ajjarapu, G. Andersson, A. Bose, C. Canizares, N. Hatziaargyriou, D. Hill, A. Stankovic, C. Taylor, T. Van, and V. Vittal, “Definition and classification of power system stability,” *IEEE Trans. Power Syst.*, vol. 19, no. 3, pp. 1387–1401, 2004.

[2] S. Greene, I. Dobson, and F. L. Alvarado, “Sensitivity of the loading margin to voltage collapse with respect to arbitrary parameters,” *IEEE Trans. Power Syst.*, vol. 12, no. 1, pp. 262–272, 1997.

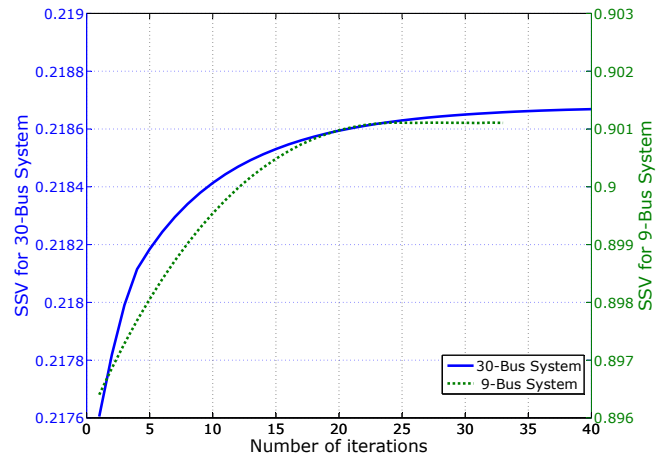


Fig. 6. Convergence of the smallest singular value to the optimum, for the 9- and 30-bus systems.

[3] R. Al Abri, E. F. El-Saadany, and Y. M. Atwa, “Optimal placement and sizing method to improve the voltage stability margin in a distribution system using distributed generation,” *IEEE Trans. Power Syst.*, vol. 28, no. 1, pp. 326–334, 2013.

[4] W. Freitas, L. C. Da Silva, and A. Morelato, “Small-disturbance voltage stability of distribution systems with induction generators,” *IEEE Trans. Power Syst.*, vol. 20, no. 3, pp. 1653–1654, 2005.

[5] J. Short, D. Infield, and L. Freris, “Stabilization of grid frequency through dynamic demand control,” *IEEE Trans. Power Syst.*, vol. 22, no. 3, pp. 1284–1293, 2007.

[6] D. Callaway, “Tapping the energy storage potential in electric loads to deliver load following and regulation, with application to wind energy,” *Energy Convers. Management*, vol. 50, pp. 1389–1400, 2009.

[7] R. J. Thomas and A. Tiranuchit, “Voltage instabilities in electric power networks,” in *18th Southeast Symp. Syst. Theory*, 1986, pp. 359–363.

[8] A. Tiranuchit and R. Thomas, “A posturing strategy against voltage instabilities in electric power systems,” *IEEE Trans. Power Syst.*, vol. 3, no. 1, pp. 87–93, 1988.

[9] A. Tiranuchit, L. Ewerbring, R. Duryea, R. Thomas, and F. Luk, “Towards a computationally feasible on-line voltage instability index,” *IEEE Trans. Power Syst.*, vol. 3, no. 2, pp. 669–675, 1988.

[10] P.-A. Lof, T. Smed, G. Andersson, and D. Hill, “Fast calculation of a voltage stability index,” *IEEE Trans. Power Syst.*, vol. 7, no. 1, pp. 54–64, 1992.

[11] I. A. Hiskens and R. J. Davy, “Exploring the power flow solution space boundary,” *IEEE Trans. Power Syst.*, vol. 16, no. 3, pp. 389–395, 2001.

[12] L. Rouco and F. Pagola, “An eigenvalue sensitivity approach to location and controller design of controllable series capacitors for damping power system oscillations,” *IEEE Trans. Power Syst.*, vol. 12, no. 4, pp. 1660–1666, 1997.

[13] J. Ma, Z. Y. Dong, and P. Zhang, “Eigenvalue sensitivity analysis for dynamic power system,” in *Int. Conf. Power Syst. Tech.* IEEE, 2006.

[14] S. Mendoza-Armenta and I. Dobson, “A formula for damping interarea oscillations with generator redispatch,” in *Proceedings of the IREP Symposium on Bulk Power System Dynamics and Control*, 2013.

[15] A. J. Wood and B. F. Wollenberg, *Power Generation, Operation, and Control*. John Wiley & Sons, 2012.

[16] J. Lavaei and S. H. Low, “Zero duality gap in optimal power flow problem,” *IEEE Trans. Power Syst.*, vol. 27, no. 1, pp. 92–107, 2012.

[17] D. K. Molzahn and I. A. Hiskens, “Convex relaxations of optimal power flow problems: An illustrative example,” *IEEE Trans. Circuits Syst. I: Reg. Papers*, vol. 63, no. 5, pp. 650–660, 2016.

[18] T. Smed, “Feasible eigenvalue sensitivity for large power systems,” *IEEE Trans. Power Syst.*, vol. 8, no. 2, pp. 555–563, 1993.

[19] R. Zimmerman, C. Murillo-Sanchez, and R. Thomas, “MATPOWER: Steady-state operations, planning, and analysis tools for power systems research and education,” *IEEE Trans. Power Syst.*, vol. 26, no. 1, pp. 12–19, Feb 2011.

[20] R. J. Avalos, C. A. Cañizares, F. Milano, and A. J. Conejo, “Equivalency of continuation and optimization methods to determine saddle-node and limit-induced bifurcations in power systems,” *IEEE Trans. Circuits Syst. I: Reg. Papers*, vol. 56, no. 1, pp. 210–223, 2009.